International Journal of Precision Engineering and Manufacturing-Green Technology (2024) 11:381–390
https://doi.org/10.1007/s40684-023-00548-x

Online ISSN 2198-0810
Print ISSN 2288-6206

REGULAR PAPER

Dry Grinding by Means of Additively Manufactured Toric Grinding Pins

Michael Keitel[1] · Berend Denkena[1] · Benjamin Bergmann[1]

Received: 20 February 2023 / Revised: 7 August 2023 / Accepted: 10 August 2023 / Published online: 26 September 2023

Abstract
The dry grinding process is challenging due to the induced thermal loads into the workpiece, which leads to a reduction of the workpiece quality. One approach to reduce the thermal loads is to adjust the grinding tool geometry by inserting a porous structure for dry grinding. This porous structure can be implemented, for example, by additively manufactured grinding tools. For this purpose, the suitability of additively manufactured vitrified cubic boron nitride grinding tools for dry grinding of tempered AISI M3:2 was investigated and compared with conventionally manufactured grinding tools to investigate the possibility of reducing the high temperatures and to verify the advantage of additively manufactured grinding tools. For this the resulting topographies and residuals stress states as well as wear of the grinding tools were analyzed. Additively manufactured grinding tools generated constant surface roughnesses of below 1 µm as well as contant compressive residual stress states. These results were attributed to a continuous self-sharpening of the grinding tools, which was shown qualitatively and quantitatively on the basis of the tool surfaces. Additively manufactured grinding tools with a porous structure thus have the potential to increase the possibilities of dry grinding.

Keywords High-speed steel 1.3344 (AISI M3:2) · Additive manufactured grinding tool · Toric grinding pins · Residual stresses · Wear behavior

1 Introduction

Fine machining by grinding is of decisive importance in the manufacture or repair of components, as this represents one of the final machining steps and thus sets the surface and subsurface properties. The surface and subsurface properties resulting from grinding determine, the application behavior of the components. In the case of forming tools, for example, the flow characteristics of the workpiece during forming are determined by the surface and subsurface properties [1]. High degrees of forming and the work hardening that occurs lead to locally different mechanical loads during forming, which result in high wear [2]. Through the final grinding process, the subsurface can be functionalized by selectively inducing compressive residual stresses in such a way as to counteract the locally occurring load stresses and thus increase the service life [3].

✉ Michael Keitel
keitel@ifw.uni-hannover.de

[1] Institute for Production Engineering and Machine Tools, Leibniz University Hannover, An der Universität 2, 30823 Garbsen, Germany

In order to be able to selectively adjust residual stresses during grinding, the separation mechanisms and, above all, the grinding power applied must be taken into account so that no thermal damage occurs. In order to prevent thermal damage to the components, cooling lubricant, mostly grinding oil, is used in large quantities during grinding [4–6]. However, the use of cooling lubricant is associated with both economic and ecological costs. Therefore, one obvious option is to dispense with cooling lubricant.

Dry grinding processes are considered problematic, as it can lead to a decrease of the workpiece quality. Basic functions such as lubrication, cleaning of the grinding tool and cooling are also omitted. Thus, there is a risk of thermal workpiece damage due to grinding burn and considerable tool wear. For this purpose, Tönshoff et al. investigated the process behavior of different cutting materials with regard to their suitability for dry grinding. High workpiece speeds of $v_{ft} = 2$ m/s were used in order to reduce heat exposure times. In internal cylindrical grinding, the potential of vitrified bonded cubic boron nitride (cBN) grinding tools to machine workpieces without negatively affecting the surface and subsurface was demonstrated. However, the wear associated with dry machining was found to be critical. As

a consequent conclusion, an optimization of the grinding wheel properties was found to be necessary [7]. Tawakoli et al. address the challenge of dry grinding by reducing the contact area to optimize friction and chip formation. By individually adjusting kinematic parameters, such as the shape of the dresser, defined structures are induced into the grinding wheel. The investigations show that the reduction of the contact area leads to comparably low cutting forces and to less heat generation. Reduced surface finishes due to the small contact area were identified as a disadvantage of this method [8]. In order to realize a dry grinding process, the heat input into the workpiece has to be reduced in order to avoid component damage. In current research, different approaches are being pursued. This paper shows the possibilities of additive manufactured (AM) grinding tools to enable a dry grinding process.

In contrast to the conventional manufacturing route, additive manufacturing of grinding tools offers the possibility of producing any grinding tool geometries close to final contour. On the one hand, this saves resources in the manufacture of grinding tools and, on the other, shortens the process times for preparing them for use, e.g. in profiling. This type of manufacturing also allows the production of geometries that were previously impossible or only possible to a limited extent using conventional manufacturing processes, and whose size can also be scaled. In the investigations presented here, toric grinding pins with a diameter of T = 30 mm were used. This shape and size of the grinding tools offers several advantages. Due to the small diameter for grinding tools, these tools can be integrated in conventional milling machines with standard tool holders and stored in the tool magazine. Furthermore, the toric geometry of the tools results in a small contact area between tool and workpiece, which reduces the heat input into the workpiece and the possibility to machine freeform surfaces in addition to plane surfaces [9, 10].

The combination of resource-saving production of the grinding tools and the possibility of integration in 5-axis machining centers with no need for cooling lubricant offers the possibility of manufacturing complex components economically and ecologically.

2 Materials and Experimental Setup

2.1 Materials

Powder metallurgical high-speed steel AISI M3:2 (ASP®2023) was used for the experimental investigations. The high-speed steel was heat treated at an austenitizing temperature of 1.400 °C by vacuum hardening followed by tempering three times at 560 °C for 1 h each time. After heat treatment, the high-speed steel has a hardness of 62 ± 2 HRC. The chemical composition of the high-speed steel is given in Table 1. The specimens used have a rectangular geometry with dimensions of 41 × 35 × 15 mm^3.

2.2 Grinding Process

2.2.1 Toric Grinding Pins

Vitrified bonded cBN toric grinding pins with a diameter of T = 30 mm and a torus radius of r_T = 5 mm were used for the investigations (Fig. 1, left). Due to the fact that there is no cooling during dry grinding and the resulting higher thermal load on the cutting grain, cBN was selected as the cutting material, since diamond tends to graphitize at high temperatures and the iron in the material might decrease this thermal transformation point even further. Two different types of tools were used. On the one hand, conventionally manufactured tools were used, and on the other hand, toric grinding pins were manufactured by an innovative additive manufacturing process by the company BDW-BINKA Diamantwerkzeug GmbH, Germany. The grit size of both tool types was d_G = 91 µm at a concentration of C = 125.

2.2.2 Grinding with Toric Grinding Pins

The grinding investigations were carried out on a CNC 5-axis milling machine tool RMF 600 DS (Röders Tec, Germany). Two different grinding strategies, lateral and frontal, are possible when grinding with toric grinding pins. The lateral grinding strategy in synchronous operation was selected here. The lateral grinding strategy is characterized by the fact that the cutting and feed directions are parallel to each other [11]. The process parameters used are summarized in Table 2.

2.3 Surface Measurements

The topographies of all tool surfaces and workpiece surfaces were measured in a field of 3 × 3 mm^2. The measurement was performed with a DUO Vario (Confovis, Germany). The surface measurements were evaluated with the software "µsoft analysis premium 8 ®" (NanoFocus AG, Germany).

For the description of tool wear, the initial condition of the tools was determined first. Subsequently, a volume

Table 1 Chemical composition of AISI M3:2

[wt %]	C	Cr	Mo	W	V	Fe
AISI M3:2	1.28	4.00	5.00	6.40	3.10	Balanced

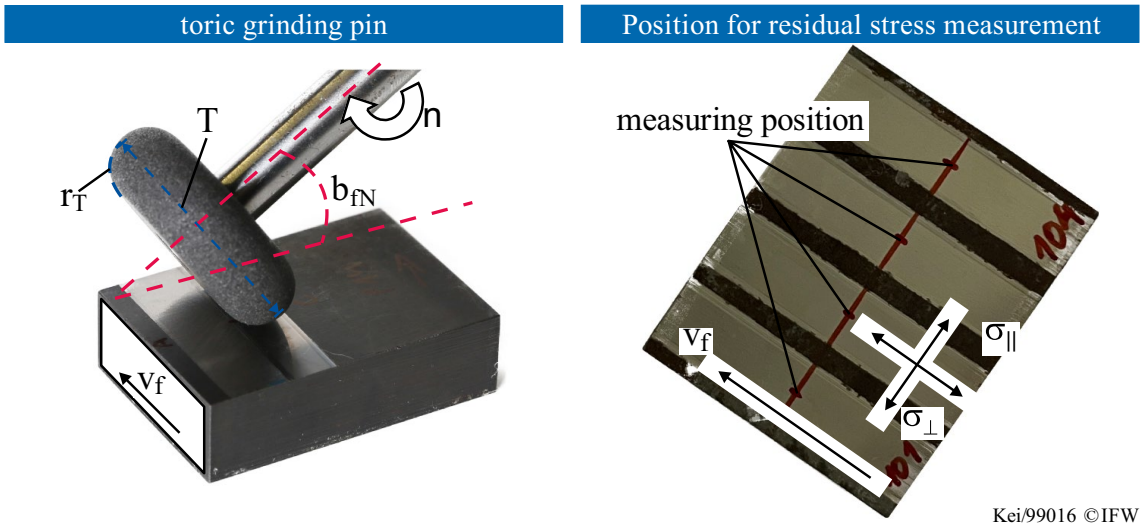

Fig. 1 Representation of a toric grinding pin(left) and positions of residual stress measurement on the specimen (right)

Table 2 Parameters of the grinding process

Parameter	Value	Unit
Cutting speed v_c	30	m/s
Feed rate v_f	500	mm/min
Depth of cut a_e	30	µm
Path distance a_b	0.104	µm
Tilt angle β_{fN}	30	°

Table 3 Specific parameters used for residual stress measurements

Anode material	Cr Kα	Specimen material	α-iron
Bragg angle 2 Θ	156.1°	Lattice plane {hkl}	{211}
Poisson's ratio	0.28	Young's modulus	220.264 [kN/mm^2]
Elastic constant ½s_2	5.81×10^{-6} [mm^2/N]	Elastic constant -s_1	1.27×10^{-6} [mm^2/N]

of $V_M = 43.05$ mm^3 was machined, as well as a reference volume of $V_{Ref} = 6.05$ mm^3 for the analysis of the surface and subsurface properties. After this defined cutting volume, the surfaces of the tools were measured at three different positions (0°, 120° and 240°) on the circumference of the tool. The wear of the tools is described by clogging and the G-ratio. The G-ratio describes the ratio between the machined volume (1) and the wear volume, whereby the wear volume is described by the radius wear (2):

$$G = \frac{V_M}{V_{T,w}} \tag{1}$$

$$V_{T,w} = \frac{90\pi}{360} * \left({r_{T,v}}^2 - {r_{T,n}}^2\right) * \pi r_{T,n} \tag{2}$$

with: $r_{T,v}$ is the torus radius before grinding$r_{T,n}$ is the torus radius after grinding, V_M is the machined volume, $V_{T,w}$ is the wear volume of the tool

2.4 Residual Stress Measurements

Residual stress measurements of the ground workpieces (Fig. 1, right) were performed by X-ray diffraction using the $\sin^2\psi$-method in ω-mode [12]. The measurements were performed on a Seifert 3003 TT dual-circuit X-ray diffractometer (GE Inspection Technologies, Germany) with a Cr-anode in combination with a V-filter and a collimator with a diameter of $d_c = 2$ mm. The applied accelerating voltage was $U_a = 30$ kV with an anode current of $I_a = 35$ mA. The information depth was $\tau = 5.5$ µm. All elastic constants and Bragg reflections used are listed in Table 3.

3 Results and Discussion

For the technological investigations on dry grinding, a total volume of $V_M = 592.2$ mm^3 was machined. With the selected process parameters, this corresponds to

a machining time of approx. 6.5 h. After a volume of $V_M = 43.05\ mm^3$, a reference surface was ground in each case, resulting in 12 reference surfaces. On these 12 reference surfaces, the surface and subsurface properties were analyzed afterwards. Furthermore, after each reference surface generated on the workpiece, the tool surfaces were measured at three different positions on the circumference confocally. The experiments were repeated with another AM toric grinding pin with same specifications. The break-off criterion was clogging on the grinding tool surface, which would lead to damage of the workpiece surface.

3.1 Tool Wear

The characterization of the toric grinding tools before and after the grinding tests, as well as after discrete cutting volumes V_M, is based on a qualitative and quantitative evaluation of the surfaces of the grinding tools in the contact area and of the torus radii. The wear behavior is further described by the G-ratio. The calculation is based on formulas (1) and (2).

Before starting the investigations, SEM images (cf. Fig. 2) and topography images (cf. Fig. 3, above) of the tool surfaces of conventionally manufactured and AM grinding tools were recorded. On the left in Fig. 2 is the conventionally manufactured grinding tool, on the right the AM grinding tool. It can be seen that the AM grinding tool has a higher porosity. The conventionally manufactured grinding tool can therefore be described as more compact/denser. The tools show no cracks, clogging or other contamination before the start of the investigations.

The tool surfaces of the two toric grinding pins in the initial state and after a machined volume of $V_M = 197.4\ mm^3$ are compared by topography images in Fig. 3. The conventionally manufactured tool is shown on the left and the AM-tool on the right. From the qualitative illustration, it can be seen that the conventionally manufactured tool already shows pronounced clogging after a machined volume of $V_M = 197.4\ mm^3$. The clogging in the contact area can be seen on the entire circumference of the tool. As it can be seen in the SEM images in Fig. 2, the conventionally manufactured grinding tool is sintered more densely and has smaller pore spaces. From this it can be concluded that the pores are clogged after a very short time. Since the grinding process is carried out dry, the lack of cooling lubricant cannot free the pores from chips. As a result, the removed chips weld with the tool surface. The resulting increased effective contact area leads to an increased temperature as a result of increased friction. Due to the massive clogging and welding, grinding burn occurred. Thus, the previously defined break-off criterion was reached. In contrast, the AM grinding tool shows only small amounts of clogging. Due to the porous structure of the AM grinding tools, a correspondingly higher volume of chips can be absorbed.

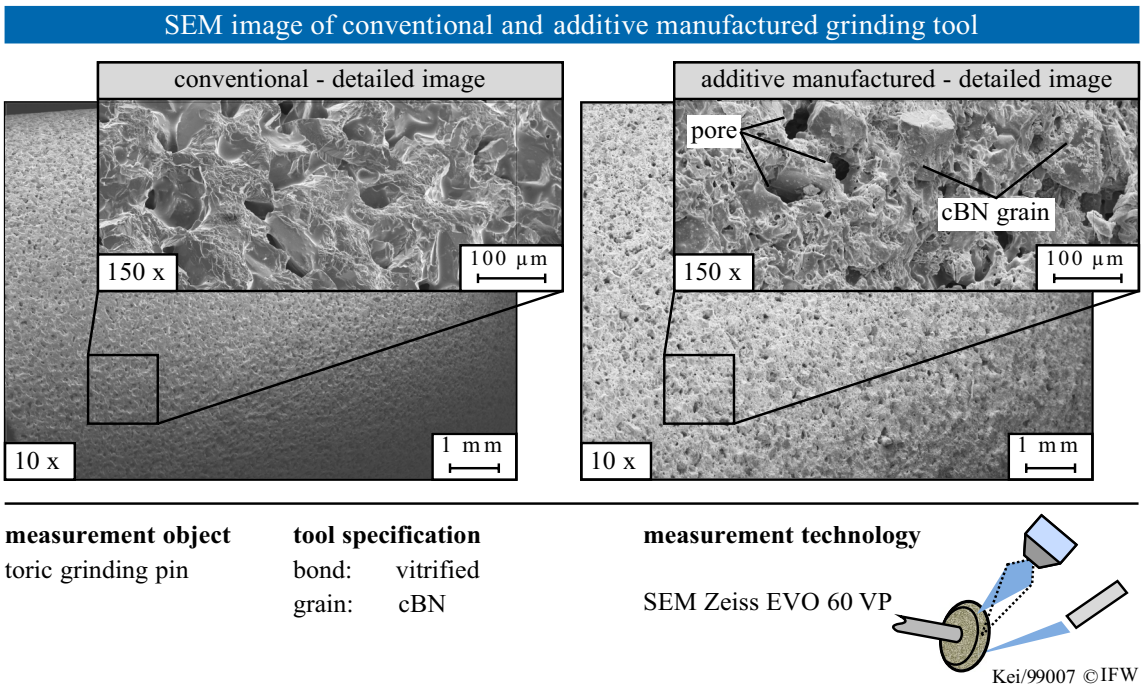

Fig. 2 SEM image of a conventional sintered and AM toric grinding pin

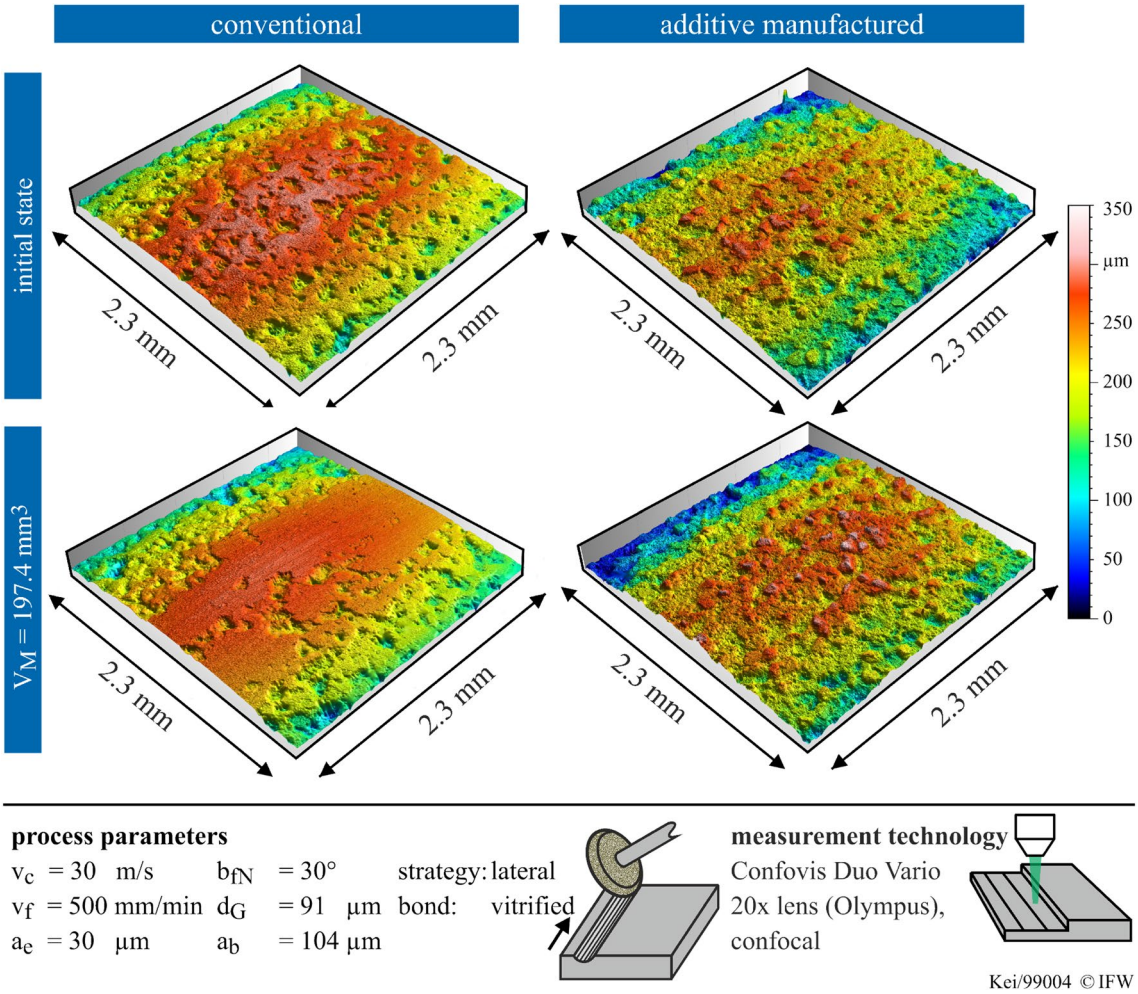

Fig. 3 Surfaces of the toric grinding pins after a machined volume of $V_M = 197.4\ mm^3$

The AM grinding tools were further used. The states of the tool surfaces after $V_M = 394.8\ mm^3$ and $592.2\ mm^3$ are shown in Fig. 4. It can be seen that the clogging of the tool surface first increases and then decreases again. After a machined volume of $V_M = 394.8\ mm^3$, the highest degree of clogging was determined. An increase in clogging with subsequent decrease indicates a self-sharpening effect. This effect is known from vitrified bonded grinding tools dressed by crushing [13]. In contrast to crushed grinding tools, where the dressing process breaks the bond, it is assumed that AM grinding tools have a coarser structure with lower bond hardness as a result of the manufacturing process. The characteristic values *Spk* and *Svk* taken from the Abbott-curve (see Fig. 4 below).

From the *Spk* value, which can be used as a measure of the grain overhang, it can be seen that the curve is constant over the entire machined volume. This indicates that there is no significant grain flattening, but rather grain splitting. The *Svk* value, which can be used as a parameter for clogging, shows an approximately constant course with fluctuations around a mean value of $Svk = 97 \pm 10\ \mu m$. This confirms the assumption that the tool surface is freed from clogging by self-sharpening.

The self-sharpening of the AM grinding tools means that clogs are continuously removed, but this is accompanied by higher radius wear. In the initial state, the conventionally manufactured grinding tool has a torus radius of $r_{T,C} = 5.027$ mm and the AM grinding tool has a torus radius of $r_{T,AM} = 5.029$ mm. After a machined volume of $V_M = 197.4\ mm^3$, the conventional grinding tool has a torus radius of $r_{T,C} = 4.96$ mm. The AM grinding tool has a torus radius of $r_{T,AM} = 4.98$ mm after a machined volume $V_M = 592.0\ mm^3$. According to formula (1) and (2), this corresponds to a G-ratio of 12.34 for the conventional grinding tool and a G-ratio of 101.7 for the AM grinding tool.

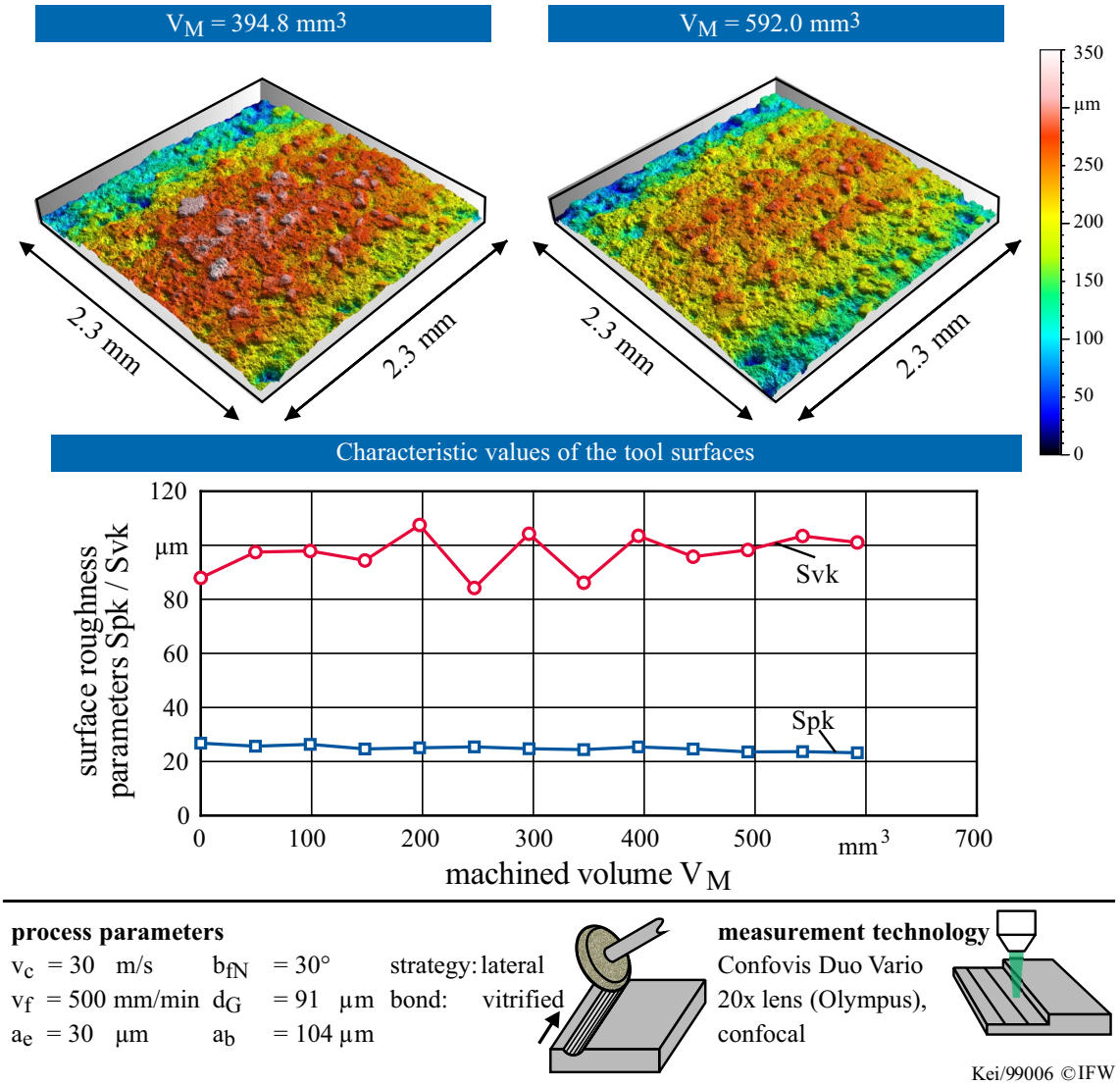

Fig. 4 Surfaces of the AM toric grinding pins after a machined volume of $V_M = 394.8$ mm^3 und $V_M = 592.0$ mm^3

3.2 Workpiece Surface

In fine-finishing machining, the resulting surface topography is of key significance. The properties of the generated surfaces significantly depend on the tool specifications and the tool condition. The resulting surfaces of the two differently manufactured grinding pin types after a machined volume of $V_M = 197.4$ mm^3 are shown in Fig. 5. Both surfaces show a wave-like structure. This results from the selected grinding strategy, in which the tool is displaced line by line by the path distance. The surface produced with the conventional grinding tool has a rougher structure and a mean arithmetic height $Sa_C = 0.822$ µm. In contrast, the surface created with the AM grinding tool has a much finer structure, which is also reflected in $Sa_{AM} = 0.598$ µm. The deviation between the two generated surfaces is thus approx. 37%.

Due to the high wear and failure of conventionally manufactured grinding tools, the surfaces of AM grinding tools are evaluated below. The resulting surfaces after a machined volume of $V_M = 394.8$ mm^3 and $V_M = 592.0$ mm^3 are shown in Fig. 6. The surfaces show roughness characteristics in a range of $Sa = 0.4$–1.1 µm after a grinding phase, where the mean arithmetic height is at a value of $Sa = 1.47$ µm. The mean value is $Sa_m = 0.71 \pm 0.22$ µm. The scatter range of approx. 30% can be attributed to continuous self-sharpening and low bond hardness and is also reflected in the *Spk* and *Svk* values shown in Fig. 4. Furthermore, these provide a reason why no grinding burn occurs on the workpiece surfaces with the AM grinding pins.

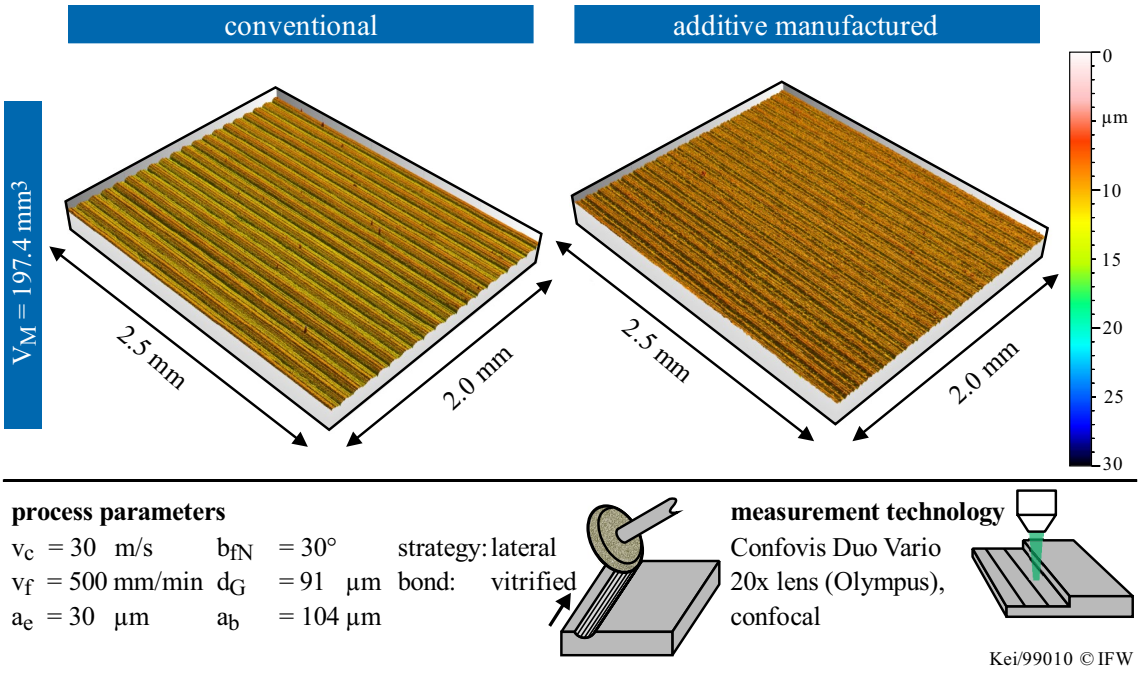

Fig. 5 Workpiece surfaces after a machined volume of $V_M = 197.4\ mm^3$

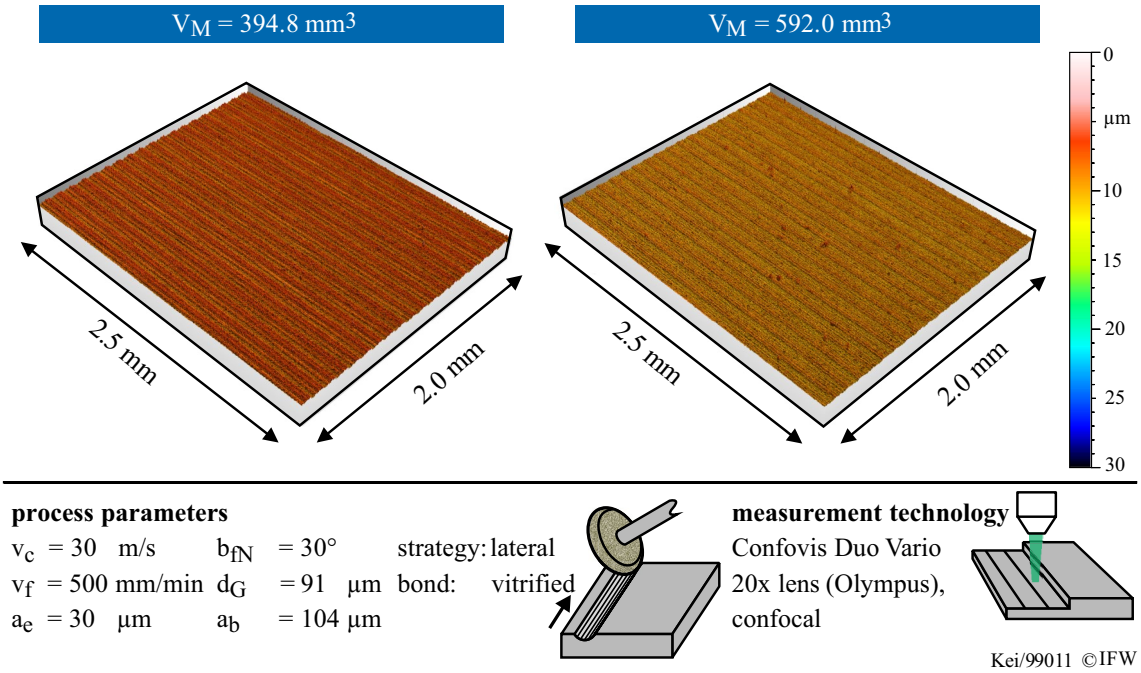

Fig. 6 Workpiece surfaces of the AM toric grinding pins after a machined volume of $V_M = 394.8\ mm^3$ und $V_M = 592.0\ mm^3$

3.3 Subsurface Properties

In order to investigate the influence of the tool specifications and the tool wear on the subsurface state, $\sin^2\psi$ residual stress measurements were performed on the reference surfaces. The results as a function of the machined volume are shown in Fig. 7. It can be seen that all grinding tools used induce compressive residual stresses in the subsurface. This can be explained by the plastic deformation due to material removal. Furthermore, a difference between the residual stresses in

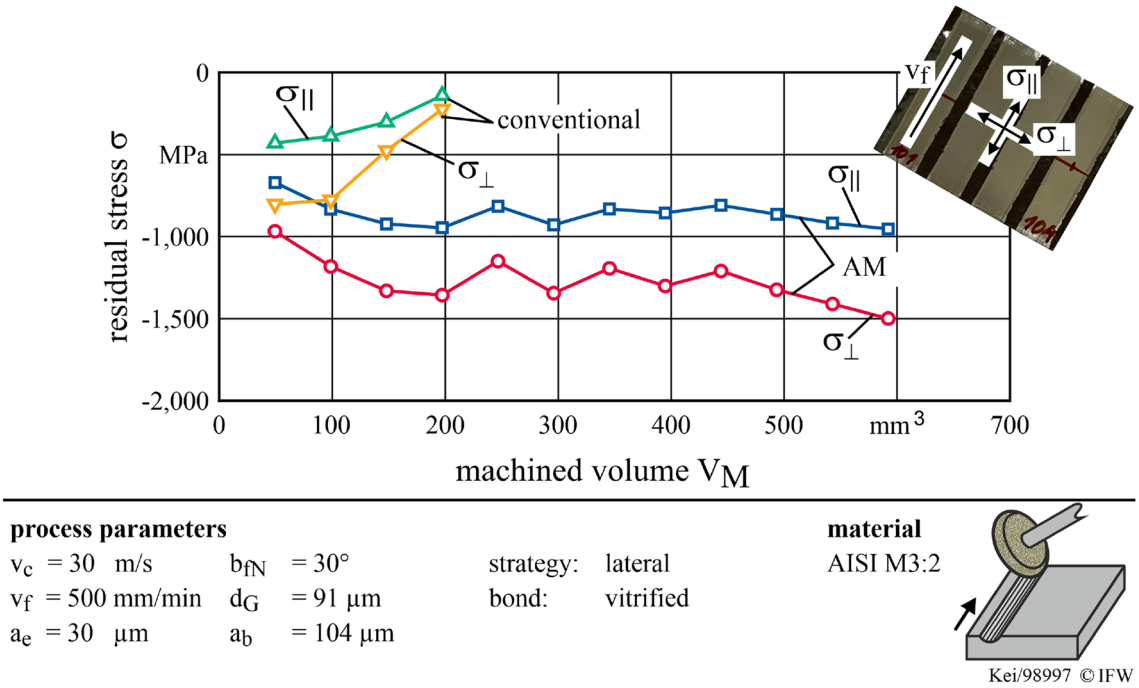

Fig. 7 Residual stress as a function of machined volume

parallel and transverse direction can be seen. In cutting direction, part of the plastically deformed material is removed again as chips, which means that the induced compressive residual stresses are lower. Transverse to the cutting direction, the material is not removed. The material which has been pressed out of the cutting path and plastically deformed remains completely intact [14]. The induced compressive residual stresses decrease with increasing machined volume when grinding with conventionally manufactured grinding tools. At a machined volume of $V_M = 197.4$ mm^3, the compressive residual stresses reach a minimum with $\sigma_{par} = -140$ MPa parallel and $\sigma_{trans} = -223$ MPa transversal to the cutting direction. The constant decrease of the induced compressive residual stresses can be explained by the continuous clogging of the pores. As shown in Fig. 3, the conventional grinding tool is almost completely clogged in the contact area. Since no free grain layer is available and the relative contact area is increased, the mechanical load on the workpiece is reduced while the thermal load increases. Conventional grinding tools, as already described in the previous section, generated grinding burn, which led to the break-off criterion being reached. In contrast, the induced compressive residual stresses of the AM grinding tools are already higher after a machined volume of $V_M = 49.35$ mm^3 by $\Delta\sigma = 240$ MPa for the parallel and by $\Delta\sigma = 165$ MPa for the transversal compressive residual stresses. Figure 7 also shows a grinding-in phase up to a machined volume of approx. $V_M = 148.05$ mm^3. From this volume on, the residual stress values fluctuate around a mean value of $\sigma_{par} = -880$ MPa or $\sigma_{trans} = -1310$ MPa. The fluctuation around these mean values can be attributed to the different degree of clogging of the grinding tool and corresponds to the opposite course of the *Svk* values. As already described in Sect. 3.1, the grinding tools are continuously clogged up to a certain degree until self-sharpening sets in and grain splitting occurs. This results in the formation of new sharp grain tips or grain breakout, which reduces the effective contact area. Until the self-sharpening effect occurs, the thermal load increases as a result of increased friction, which leads to a decrease in the compressive residual stresses. The maximum induced compressive residual stresses are parallel to the cutting direction at $\sigma_{par} = -952.9 \pm 12.3$ MPa and transversal to the cutting direction at $\sigma_{trans} = -1498.3 \pm 76.8$ MPa.

4 Summary

The prevention of high thermal workpiece stress and resulting workpiece damage represents the major challenge to realize a dry grinding process. Previous studies on dry grinding have shown that both the grinding process and the grinding tool specifications must be adapted to deal with these challenges. Therefore, the aim of the investigations presented in this paper was to demonstrate the general suitability of additive manufactured grinding tools for dry grinding. For this objective, conventionally manufactured vitrified grinding pins and additive manufactured vitrified grinding pins were used for grinding a hardened high-speed steel (AISI M3:2). The evaluation of

the performance was done on the basis of tool surfaces, the G-ratio, the workpiece surface produced and the residual stresses induced in the workpiece. The results of the investigations are as follows:

Tool wear The conventionally manufactured grinding tool shows pronounced clogging and welding, leading to grinding burn and failure. In contrast, the additive manufactured (AM) grinding tool exhibits lower clogging due to its porous structure, allowing for higher chip absorption. The AM tools show self-sharpening, with clogging being continuously removed, resulting in higher radius wear. The G-ratio for the conventional tool is 12.34, while for the AM tool it is 101.7.

Workpiece surface The surfaces generated by the conventional grinding tool are rougher compared to those produced by the AM tool. The mean arithmetic height for the conventional tool is 0.822 µm, while for the AM tool it is 0.598 µm, representing a difference of approximately 37%.

Subsurface properties Both the conventional and AM grinding tools induce compressive residual stresses in the subsurface. The compressive residual stresses decrease with increasing machined volume for the conventional tool due to continuous clogging of the pores. In contrast, the AM grinding tools exhibit higher induced compressive residual stresses, with fluctuations around mean values of $\sigma_{par} = -880$ MPa or $\sigma_{trans} = -1310$ MPa. The fluctuation is attributed to the varying degree of clogging and corresponds to the changes in the tool's surface characteristics.

Overall, the results indicate that the AM grinding tools have advantages in terms of reduced clogging, self-sharpening, and higher compressive residual stresses. However, the AM tools also experience higher radius wear. Further investigations are needed to optimize the bond hardness and to investigate the influence of process parameters and tool specifications on surface and subsurface properties.

Acknowledgements The authors gratefully acknowledge BDW-BINKA Diamantwerkzeug GmbH for the grinding tools and the German Research Foundation (DFG) for the founding of the subproject T09 "On-site processing of complex and cost-intensive capital goods" of the Transregional Collaborative Research Centre on sheet-bulk metal forming (TCRC73).

Author Contributions BD reviewed and edited the manuscript together with BB. MK developed the concept of this work, conducted the experiments, analyzed the data and wrote the manuscript.

Funding Open Access funding enabled and organized by Projekt DEAL.

Data availability The data cannot be released due to a project agreement with the partners involved.

Declarations

Conflict of interest On behalf of all authors, the corresponding author declares that there is no conflict of interest. The supply of the tools by the named manufacturer takes place in the context of a common, by the German Research Foundation (DFG) promoted co-operation project.

References

1. Wagner, R., Völkl, R., & Engel, U. (2008). Tool life enhancement in cold forging by locally optimized surfaces. *Journal of Materials Processing Technology, 201*(1–3), 2–8. https://doi.org/10.1016/j.jmatprotec.2007.11.152
2. Lange, K., Hettig, A., & Knörr, M. (1992). Increasing tool life in cold forging through advanced design and tool manufacturing. *Journal of Materials Processing Technology, 35*(3–4), 495–513. https://doi.org/10.1016/0924-0136(92)90337-R
3. Altan, T., Blaine, L., & Yen, Y. C. (2001). Manufacturing of dies and molds. *CIRP Annals-Manufacturing Technology, 50*(2), 404–422. https://doi.org/10.1016/S0007-8506(07)62988-6
4. Klocke, F., Brinksmeier, E., & Weiner, K. (2005). Capability of hard cutting and grinding processes. *CIRP Annals-Manufacturing Technology, 54*(2), 22–45. https://doi.org/10.1016/S0007-8506(07)60018-3
5. Kermouche, G., Rech, J., Hamdi, H., & Bergheau, J. M. (2010). On the residual stress field induced by a scratching round abrasive grain. *Wear, 269*(1–2), 86–92.
6. Heinzel, C., Sölter, J., Jermolajev, S., Kolkwitz, B., Brinksmeier, E. (2014). A versatile method to determine thermal limits in grinding. In: 2nd CIRP 2nd CIRP Conference on Surface Integrity (CSI), *CIRP Procedia 13*, 131–136.
7. Tönshoff, H. K., Wobker, H.-G., Brunner, G., & Kroos, F. (1995). Möglichkeiten und Grenzen des Trockenschleifens gehärteter Stähle. *HTM, 50*, 78–84.
8. Tawakoli, T., Westkaemper, E., & Rabiey, M. (2007). Dry grinding by special conditioning. *The International Journal of Advanced Manufacturing Technology, 33*, 419–424. https://doi.org/10.1007/s00170-006-0770-5
9. Denkena, B., de Leon, L., & Behrens, L. (2010). Contact conditions in 5-axis-grinding of double curved surfaces with toric grinding wheels. *Advanced Material Research, 126–128*, 56–56.
10. Tönshoff, H. K., Böß, V., & Urban, B. (2002). Schleifen im Werkzeug- und Formenbau. *Jahrbuch Schleifen, Honen, Läppen und Polieren, 60*, 161–171.
11. Grove, T., Lucas, H., & Denkena, B. (2018). Residual stresses in grinding of forming tools with toric grinding pins. *Procedia CIRP, 71*, 354–357. https://doi.org/10.1016/j.procir.2018.05.040
12. Müller, P., & Macherauch, E. (1961). Das sin2(ψ)-Verfahren der röntgenographischen Spannungsmessung. *Angewandte Physik, 13*, 305–312.
13. Denkena, B., Krödel-Worbes, A., Keitel, M., & Wolters, P. (2021). Influence of dressing strategy on tool wear and performance behavior in grinding of forming tools with toric grinding pins. *Production Engineering, 16*, 513–522. https://doi.org/10.1007/s11740-021-01089-5

14. Denkena, B., Grove, T., & Lucas, H. (2015). Influences of grinding with toric CBN grinding tools on surface and subsurface of 1.3344 PM steel. *Journal of Materials Processing Technology, 229*, 541–548. https://doi.org/10.1016/j.jmatprotec.2015.09.039

Michael Keitel received a Bachelor's and a Master's degree in mechanical engineering from Leibniz University of Hanover. He is currently a research associate at the Institute of Production Engineering and Machine Tools (IFW) with a focus on dry grinding.

Prof. Dr.-Ing. Berend Denkena obtained his Ph.D. from the University of Hanover. After his Ph.D. he worked in industrial sectors like construction an machine tools. In 2001 he appointed Professor for Production Engineering and Machine Tools. His research is focused on manufacturing processes and machine tools, such as technologies for autonomous machine tools.

Dr.-Ing. Benjamin Bergmann earned his doctorate in mechanical engineering on cutting edge roundings from the University of Hannover. Currently he is head of Department "Manufacturing Processes", Institute of Production Engineering and Machine Tools (IFW), Leibniz Universität Hannover. His research topics are manufacturing processes with a focus on tool development.